Extremophiles (2003) 7:353–360
DOI 10.1007/s00792-003-0330-y

ORIGINAL PAPER

Rob J. Frankenberg · Maria Andersson
Douglas S. Clark

Effect of temperature and pressure on the proteolytic specificity of the recombinant 20S proteasome from *Methanococcus jannaschii*

Received: 20 September 2002 / Accepted: 17 March 2003 / Published online: 18 June 2003

Abstract The hydrolytic specificity of the recombinant 20S proteasome from the deep-sea thermophile *Methanococcus jannaschii* was evaluated toward oxidized insulin B-chain across a range of temperatures (35°, 55°, 75°, and 90°C) and hydrostatic pressures (1, 250, 500, and 1,000 atm). Of the four temperatures considered, the same maximum overall hydrolysis rate was observed at both 55° and 75°C, which are much lower than the T_{opt} of 116°C previously observed for a small amide substrate (Michels and Clark 1997). At 35°C the rates of cleavage were highest at the carboxyl side of glutamine and leucine, whereas at the three higher temperatures, the most rapid cleavages occurred after leucine and glutamic acid residues. The distribution of proteolytic fragments and the cleavage sequence also varied between the lowest and higher temperatures. Application of hydrostatic pressure did not increase proteasome activity, as observed previously for the amide substrate (Michels and Clark 1997), but instead significantly reduced the overall conversion of the polypeptide substrate. Overall cleavage patterns observed for the recombinant *M. jannaschii* proteasome were similar to those reported previously for *Thermoplasma acidophilum* (Akopian et al. 1997) and human proteasomes (Dick et al. 1991), indicating that proteasome specificity has been conserved despite significant environmental diversity.

Communicated by G. Antranikian

R. J. Frankenberg
Bayer Health Care, Berkeley, California, USA

M. Andersson
Department of Biotechnology, University of Lund, Lund, Sweden

D. S. Clark (✉)
Department of Chemical Engineering, University of California,
201 Gilman Hall, Berkeley, CA, 94720, USA
E-mail: clark@cchem.berkeley.edu
Tel.: +1-510-6422408
Fax: +1-510-6431228

Keywords High pressure · Hydrolytic specificity · *Methanococcus jannaschii* · Thermophilic proteasome

Introduction

The 20S proteasome is a large protein complex (650–750 kD) found in several organisms ranging from eukaryotes to archaea. It is responsible for the non-lysosomal proteolytic degradation (McGuire and DeMartino 1989) of denatured (Murakami et al. 1992) and ubiquitin-tagged proteins (Seufert and Jentsch 1992). X-ray crystallography of the 20S proteasome from the thermophilic archaeon *Thermoplasma acidophilum* (*Ta*) revealed that the 20S proteasome is composed of 28 subunits arranged in four, seven-membered rings (Lowe et al. 1995). The rings stack to form a longitudinally elongated barrel sequestering the 14 active-site threonines along the inner circumference of β-rings within the proteasome (Lowe et al. 1995). Eukaryotic proteasomes may have up to 14 sequentially distinct subunits (Chen and Hochstrasser 1995), while archaeal proteasomes contain only two, the α and β. The reduced complexity of the archaeal system has facilitated the functional expression of several recombinant proteasomes, including those from the thermophiles *Ta* (Zwickl et al. 1992), *Methanosarcina thermophila* (Maupin-Furlow et al. 1998), and *Methanococcus jannaschii* (*Mj*) (Wilson et al. 2000). However, in at least one case, *M. jannaschii*, the recombinant thermophilic proteasome expressed in *E. coli* did not exhibit native-like enzymatic properties without denaturation and high-temperature refolding (Frankenberg et al. 2001).

Broad proteolytic specificity is one of the most striking properties of proteasomes. Studies with small (3–5 residue) peptide substrates indicate that eukaryotic proteasomes display five distinct proteolytic activities: chymotryptic, tryptic, peptidyl-glutamyl hydrolytic, cleavage after branched-chain amino acids, and cleavage between small neutral amino acids. However, only the

first three activities have been demonstrated in archaeal proteasomes. The *Ta* 20S proteasome cleaves preferentially after large hydrophobic groups, and also exhibits appreciable tryptic and peptidyl-glutamyl hydrolytic activity (Akopian et al. 1997).

Proteasome activity against small (up to 4 amino acid residues) amide substrates has been enhanced up to fourfold by the addition of low concentrations of detergents (SDS) (Rubin and Finley 1995), denaturants (guanidinium chloride) (Yamada et al. 1995), divalent salts ($MnCl_2$) (Akopian et al. 1997), and the application of high pressure (Michels and Clark 1997). Chemical activating agents have also been studied in conjunction with modulation of eukaryotic proteasome specificity (Yamada et al. 1995, 1998). For example, Djaballah and coworkers found that changes to the solution properties (e.g., increased salt concentration or introduction of denaturants) could either enhance or eliminate certain proteolytic activities with a concomitant change in the proteasome's sedimentation velocity (Djaballah et al. 1993). The authors concluded that minor changes in sedimentation velocity reflected conformational changes that may be associated with variations in proteolytic specificity.

Conformational fluctuations may also be responsible for variations in substrate specificity; however, manipulation of in vitro solution composition cannot duplicate in vivo conditions. The isolation, characterization, and cloning of the 20S proteasome from the deep-sea hyperthermophile *Mj* presents an unusual opportunity to study proteolytic specificity as a function of two adjustable and biologically relevant parameters, temperature and hydrostatic pressure. Pressure is particularly intriguing, given that *Mj* displayed a barophilic response in previous growth experiments (Miller et al. 1988), and its proteasome exhibited enhanced activity and thermostability toward Cbz-Ala-Ala-Leu-pNA upon application of pressure (Michels and Clark 1997). Temperature and pressure are thus important determinants of the *Mj* proteasome's activity, and varying these conditions in vitro may enable some degree of control over the proteasome's proteolytic specificity. Building on previous work performed with proteasomes and oxidized insulin B-chain (B_{ox}) (Dick et al. 1991; Wenzel et al. 1994), we have probed the specificity of the recombinant 20S *Mj* proteasome (r20S*Mj*p) as a function of temperature and pressure.

Materials and methods

Purification of the recombinant 20S *Mj* proteasome (r20S*Mj*p)

Recombinant 20S *Mj* proteasome was purified as described previously (Frankenberg et al. 2001). Briefly, crude lysates of *E. coli* expressing the α and β subunits of the *Mj* proteasome were individually heat-purified at 70°C for 120 min. After centrifugation, 4 M urea was added to the supernatants, which were incubated at room temperature for 1 h. The samples were dialyzed into zymogram-developing buffer (50 mM Tris, 200 mM NaCl, 5 mM $CaCl_2$, $pH_{20°C} = 8.72$; $pH_{85°C} = 7.5$) at 85°C for 1 h. Clarified supernatant contained assembled proteasome with native-like properties (Frankenberg et al. 2001). Proteasome activity was verified by hydrolysis of Cbz-Ala-Ala-Leu-pNA at 95°C. Total protein was measured by the BCA assay (Pierce, Rockford, IL). The r20S*Mj*p preparation was stored at −80°C in zymogram buffer at a protein concentration of 0.8 mg/ml.

Temperature digests of insulin B_{ox}

1 mg/ml bovine insulin B_{ox} (Sigma, St. Louis, MO) was dissolved in reaction buffer (50 mM Tris, 5 mM $CaCl_2$, 1 mM dithiothreitol) adjusted to pH 7.5 at the appropriate reaction temperature ($pH_{20°C} = 7.82$ for 35°; $pH_{20°C} = 8.18$ for 55°; $pH_{20°C} = 8.54$ for 75°; $pH_{20°C} = 8.81$ for 90°C). 500-µl aliquots of the insulin solution were transferred to 1.5-ml Eppendorf microfuge tubes and preheated for 45 min at the desired reaction temperature. 25 µl of thawed proteasome solution was added to the preheated solution and allowed to incubate for 0, 10, 20, 30, 60, 120, 360, 720, and 1,440 min. After each incubation period, 50 µl of formic acid was added to each sample to stop the digestion. The sample was centrifuged at 14,000 r.p.m. to remove particulates, and transferred to silanized Target DP HPLC vials.

High-pressure digests of insulin B_{ox}

Sample preparation was the same as for the temperature digests. Samples of 1.25 ml of insulin B_{ox} solution and 62.5 µl of proteasome solution were loaded into 500-µl polypropylene transfer pipette bulbs (Samco, San Fernando, CA) and sealed with heated tongs. Ambient-pressure control samples were produced as above. Sample vessels were loaded into a 35°C high-pressure reactor assembly (Model No. R1-6-100; High Pressure Equipment Company, Erie, PA) and pressurized to 250, 500, and 1,000 atm with a hydrostatic pressure generator (Model No. 31–5.75–75; High Pressure Equipment Company). Samples were incubated for 12 h under pressure, quenched with 125 µl of formic acid, centrifuged, and transferred to vials for LC/MS analysis.

LC/MS analysis of insulin B_{ox} digests

LC/MS was conducted using Agilent Technology's Series 1100 Tandem LC/MS system. Reverse-phase liquid chromatography (RPLC) was performed at 30°C on each of the digests using a Jupiter 5-µm C18 300A column (250×4.60 mm, Phenomenex, Torrance, CA). Each sample (25 µl) was applied to the column preequilibrated with a buffer comprising 40 mM acetic acid and 19 mM ammonium hydroxide. Peptides were eluted with an acetonitrile gradient to 43% over 50 min. In-line API-ES mass spectroscopy was carried out with the following control settings: drying gas (N_2), 12 L/min at 350°C; nebulizer pressure, 56 bar; capillary voltage, 4,000 V. ChemStation analysis software including deconvolution macros and Peptide Tools modules (Agilent Technologies, Palo Alto, CA) was used to sequence degradation fragments by most abundant molecular weight determination. Peak areas were calculated from total ion chromatographs using buffer component peaks as internal standards. Control experiments performed under all conditions without the presence of proteasome were also analyzed by LC/MS to ensure that insulin did not degrade or precipitate from solution at high temperatures and pressure. All such controls were negative, indicating that insulin degradation was induced by the proteasome in all cases.

Results

Temperature effects on proteolysis of B_{ox} by r20S*Mj*p

Comparison of mass spectroscopy total ion chromatographs (MS TIC) of B_{ox} solutions with and without

r20S*Mj*p revealed significant levels of proteolysis at all assay temperatures. The distribution and identity of the proteolytic fragments were similar for samples incubated at 55°, 75°, and 90°C. However, the 35°C TIC contained numerous fragments that were not present at higher temperatures. Figure 1 displays a representative TIC profile for 35° and 75°C.

Samples were incubated for 1,440 min and several time points were taken at each temperature for LC/MS analysis during this period. For the majority of resolved peaks, the peak area grew at a constant rate before nearing a plateau at longer (~120–360 min) incubation times. However, the areas of a few peaks grew at a constant rate for early time periods, and then receded at later times. For example, at 75°C the area of the peak resolved at ~18.0 min stopped increasing after 120 min, and receded after 360 min. Other receding peaks at 75°C were observed at retention times of ~21.5 and ~34.3 min. Concomitantly, other peaks only appeared after longer (> 360 min) incubation times. For example, at 35°C the peak at ~7.1 min appeared only after 360 min.

The deconvolution and peak identification results are summarized in Tables 1 and 2. Peak identifications were made prior to any cleavage-site assignments. Order-of-appearance rankings, starting with one, were assigned by noting the incubation time of the first appearance of a peak at a particular retention time. Peaks appearing earlier in the degradation reactions are assigned lower numbers. The number of cleavable sites, the average length of digested fragments, and the number of fragments generated for 35° and 75°C are summarized in Table 3. On average, shorter peptides were produced at the higher temperatures. The majority of these short peptides were generated from the C-terminal end of the substrate (Fig. 2). A few of the longer peptides observed at longer reaction times are consistent with the products of possible plastein, or transpeptidation, reactions, although to our knowledge no such reactions have been previously observed with a proteasome.

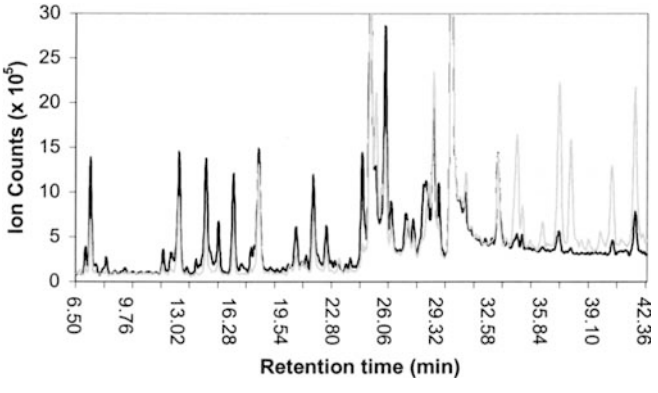

Fig. 1 Total ion chromatographs comparing the peptide profiles of B_{ox} by r20S*Mj*p. *Gray and black lines* represent profiles for samples incubated for 720 min at 35° and 75°C, respectively. The peak at ~41.5 min corresponds to undigested B_{ox} whereas peaks at ~25 and ~30 min are constant peaks present in blank runs with the buffered B_{ox} solution

In addition to single time-point analyses, kinetic data were obtained by assaying individual samples at multiple time points. Measurement of the total ion counts under each TIC peak allowed qualitative rate comparisons for consumption of B_{ox} and the production of proteolytic fragments. The time required to achieve 50% conversion for the 55° and 75°C digestions were nearly identical at ~325 min, whereas the 90° and 35°C samples reached this point at ~400 and ~800 min, respectively (data not shown). For 75°C samples, the rate of formation for each fragment appearing at 10 min was evaluated for repeated incubations. The highest formation rates at 75°C were found to correspond to the sequences VCGERGFFYTPKA (residues 18–30) and ALYL (14–17). These fragments were produced rapidly at the onset of the incubation at nearly the same rates. Complementary fragments were produced at lower rates, e.g., the production of FVNQHLCG (1–8) was followed by SHLVE (9–13) (Fig. 3).

After incubation for 10 min at 35°C only two fragments, FVNQHLCG (1–8) and VCGERGFFYTPKA (18–30), were observed. SHLVEALYL (9–17), ALYLVCGERGFFY (14–26), and HLCGSHLVEALYL (5–17) were observed only after 20 min (Fig. 4).

Degradation products of the fragment SHLVEALYL (9–17) were initially observed only at 75°C. Overall, the highest rates observed for peaks appearing early in the degradation reaction were observed at 75°C.

Based on the rate data, reaction sequences were proposed and cleavage preferences were assigned for each temperature. At 75°C, $k_L{}^{17}\text{-}_V{}^{18}$ (where $k_L{}^{17}\text{-}_V{}^{18}$ represents the cleavage rate between Leu 17 and Val 18) $\sim k_E{}^{13}\text{-}_A{}^{14} > k_G{}^{8}\text{-}_S{}^{9}$ and at 35°C $k_G{}^{8}\text{-}_S{}^{9} \sim k_L{}^{17}\text{-}_V{}^{18} > k_Q{}^{4}\text{-}_H{}^{5} \sim k_E{}^{13}\text{-}_A{}^{14} \sim k_Y{}^{26}\text{-}_T{}^{27}$. The cleavage sequence at 35°C was easier to decipher due to the smaller number of overlapping fragments (Fig. 2). At lower temperatures, the peptidyl glutamyl hydrolase activity was preferred, while at higher temperatures this activity was not observed until significantly longer incubation times.

Pressure effects on r20S*Mj*p proteolysis of B_{ox} at 35°C

Comparison of the percentage conversion of B_{ox} at 35°C and 1, 250, 500, and 1,000 atm of hydrostatic pressure revealed a significant decrease in all proteolytic activity at elevated pressures (Fig. 5). The peak profiles for pressurized degradation reactions at 35°C were identical but diminished in area relative to reactions performed at ambient pressure. No new fragments or unique cleavages were observed as a result of pressurization.

Discussion

Temperature optima and cleavage specificity

The temperature of optimum activity (T_{opt}) for r20S*Mj*p (Frankenberg et al. 2001) and native 20S *Mj* proteasome

Table 1 Peak assignments for LC/MS peaks resolved from all samples incubated at 35°C. The retention time is followed by the deconvoluted molecular weight obtained from the peak. The calculated molecular weight is the most abundant molecular weight for the assigned peptide. The order of appearance parameter indicates how early in the incubation period that fragment appeared. *1* corresponds to peaks appearing at $t \geq 10$ min; *2* corresponds to peaks appearing at $t \geq 20$ min, etc., for the time points 10, 20, 30, 60, 120, 360, 720, and 1,440 min. The length refers to the number of residues in that fragment

Retention time (min)	Actual deconvoluted MW (Da)	Calculated fragment MW (Da)	Sequence	Order of appearance	Length (residues)
3.33	122.2	121.1	Tris	B	
4.78	315.2	315.2	PKA	6	3
7.11	668.2	668.3	VCGERG	6	6
	477.2	477.2	HLCG		4
7.42	416.3	416.2	TPKA	4	4
	315.2	315.2	PKA		3
8.42	356.3	356.2	SHL		3
12.01	579.3	579.3	YTPKA	6	5
12.52	247.3	247.1	VE		2
	219.1	219.1	EA		2
13	507.2	507.2	FVNQ	3	4
	360.2	360.2	LVE		3
	247.1	247.1	VE		2
14.71	584.3	584.3	SHLVE	4	5
15.5	815.3	815.3	VCGERGF	6	6
	663.2	663.3	CGSHLV		6
16.45	655.4	655.3	FYTPK	5	5
18.04	965.5	965.4	FVNQHLCG	1	7
20.01	757.4	757.4	FVNQHL	6	6
20.43	726.3	726.4	FYTPKA	6	6
21.06	905.3	905.4	LCGSHLVE		8
21.49	1,042.4	1,042.4	VNQHLCGSH	4	9
22.31	1,113.5	1,113.5	HLCGSHLVEA	6	10
23.12	1,302.7	1,302.6	FVNQHLCGSHL	6	11
24.59	768.5	768.4	SHLVEAL	6	7
	408.2	408.2	LYL		3
	295.3	295.2	LY		2
25.43	1,530.7	1,530.7	FVNQLCGSHLVE	5	12
26.03	479.3	479.3	ALYL	5	4
26.44	1,128.5	1,128.5	ALYLVCGERG	4	10
	962.5	962.4	VCGERGFF		8
27.46	873.5	873.4	FFYTPKA	4	7
27.81	931.4	931.5	SHLVEALY	6	8
	707.4	707.3	LVEALY		6
	413.1	413.2	GSHL		4
28.74	1,423.6	1,423.6	CGERGFFYTPKA	3	12
	1,026.3	1,026.4	CGERGFFY		7
29.07	1,522.7	1,522.7	VCGERGFFYTPKA	1	13
	1,125.5	1,125.5	VCGERGFFY		9
29.39	578.3	578.3	ALYLV	6	5
31.07	1,714.7	1,714.8	EALYLVCGERGFFY	4	14
33.09	905.6	905.4	VNQHLCGS		8
	569.5	569.2	CGERG		5
34.3	1,044.5	1,044.6	SHLVEALYL	2	9
	913.4	914.3	HLCGSHLV		8
34.64	1,401.7	1,401.5	YLVCGERGFFY	5	11
	1,044.5	1,044.4	EALYLVCGE		9
36.94	1,502.8	1,502.7	HLCGSHLVEALYL	2	13
37.68	1,585.8	1,585.8	ALYLVCGERGFFY	2	13
40.26	2,548.3	2,549.2	SHLVEALYLVCGERGFFYTPKA	4	22
41.69	1,748.3	1,748.8	FVNQHLCGSHLVEALYLVCGERGFFYTPKA [+2]	B	30

(n20S*Mj*p) (Michels and Clark 1997) against the small colorimetric substrate Cbz-Ala-Ala-Leu pNA was significantly higher ($T_{opt} \sim 115$°C) than that observed for the degradation of the larger protein-like polypeptide B_{ox} by r20S*Mj*p ($T_{opt} < 90$°C). The difference in these optima might be explained by the physiological relevance of the substrate (i.e., the polypeptide insulin more closely resembles the majority of protein substrates acted upon by the proteasome during its normal physiological function). The proteasome has evolved as a cytosolic protein-degrading complex with compartmentalized active sites. The regulation of access to the active regions must be stringent to sequester its proteolytic activity. Hydrophobic loops protruding into the 1.3 nm

Table 2 Peak assignments for LC/MS peaks resolved from all samples incubated at 75°C. The retention time is followed by the deconvoluted molecular weight obtained from the peak. The calculated molecular weight is the most abundant molecular weight for the assigned peptide. The order of appearance parameter indicates how early in the incubation period that fragment appeared. *1* corresponds to peaks appearing at $t \geq 10$ min; *2* corresponds to peaks appearing at $t \geq 20$ min, etc., for the time points 10, 20, 30, 60, 120, 360, 720, and 1,440 min. The length refers to the number of residues in that fragment

Retention time (min)	Actual deconvoluted MW (Da)	Calculated fragment MW (Da)	Sequence	Order of appearance	Length (residues)
3.34	121.2	121.1	Tris		
4.83	315.2	315.2	PKA	5	3
7.12	668.3	668.3	VCGERG	4	6
	477.2	477.2	HLCG		4
7.42	416.3	416.2	TPKA	1	4
8.42	356.1	356.2	SHL	5	3
12	579.3	579.3	YTPKA	4	5
13	507.4	507.3	Y\LYLV	1	4
14.7	584.3	584.3	SHLVE	1	5
15.5	815.3	815.3	VCGERGF	2	6
16.44	566.4	566.3	FYTPK	1	5
16.98	634.3	634.3	GFFYT	6	5
17.55	366.2	366.2	ALY	4	3
17.75	814.4	814.3	HLCGSHL		7
	720.3	720.3	NQHLGC		6
18.02	965.5	965.4	FVNQHLCG	1	8
20.38	726.3	726.4	FYTPKA	3	6
20.83	1,042.6	1,042.5	HLCGSHLVE	3	9
21.05	1,042.4	1,042.4	VNQHLCGSH	4	9
	905.5	905.4	LCGSHLVE		8
21.47	1,042.4	1,042.4	VNQHLCGSH	1	9
22.31	1,113.5	1,113.5	HLCGSHLVEA	2	10
22.86	1,092.3	1,092.5	YLVCGERGF	6	9
23.5	1,125.3	1,125.3	VCGERGFFY	6	9
	1,070.4	1,070.4	LVEALYLVC		9
24.57	408.2	408.2	LYL	1	3
	295.3	295.3	LY		2
26.02	479.3	479.3	ALYL	1	4
26.39	962.5	962.5	VCGERGFF	2	8
	712.4	712.4	GSHLVEA		7
27.31	873.5	873.4	FFYTPKA	4	7
27.79	707.5	707.4	VEALYL	2	6
	413.1	413.2	GSHL		4
28.44	507.4	507.3	LYLV		4
28.62	1,423.6	1,423.6	CGERGFFYTPKA	1	12
29.08	1,522.7	1,522.7	VCGERGFFYTPKA	1	13
	944.5	944.4	YLCGERG		7
29.39	578.3	578.3	ALYLV	1	4
30.81	1,190.4	1,190.5	FVNQHLCGSH		10
31.07	1,238.6	1,238.5	LVCGERGFFY	1	10
33.09	905.8	905.4	VNQHLCGS		8
	569.5	569.2	CGERG		5
34.31	1,044.5	1,044.6	SHLVEALYL	1	9
34.64	1,401.5	1,401.5	YLVCGERGFFY	1	11
	577.4	577.3	FFYT		4
36.15	1,272.5	1,272.6	GERGFFYTPKA	6	11
41.67	1,748.4	1,748.8	FVNQHLCGSHLVEALYLVCGERGFFYTPKA [+2]		30

Table 3 Summary of results from B_{ox} degradation by r20S*Mj*p at 35° and 75°C, respectively, after a total incubation time of 1,440 min

Temperature	Number of sites cleaved	Number of fragments generated	Average fragment length
35°C	22	49	7.1 ± 4
75°C	23	45	6.7 ± 2.8

α-ring annulus of the r20S *Ta* proteasome (r20S*Ta*p) (Lowe et al. 1995) only allow access by denatured protein substrates destined for turnover. In general, the "bite and chew" (Kisselev et al. 1999) and "bread slicer" (Akopian et al. 1997) mechanisms proposed for proteasomal action involve complex interactions between the protein substrate and the interior cavity of the proteasome. These interactions, specific to a given substrate, its

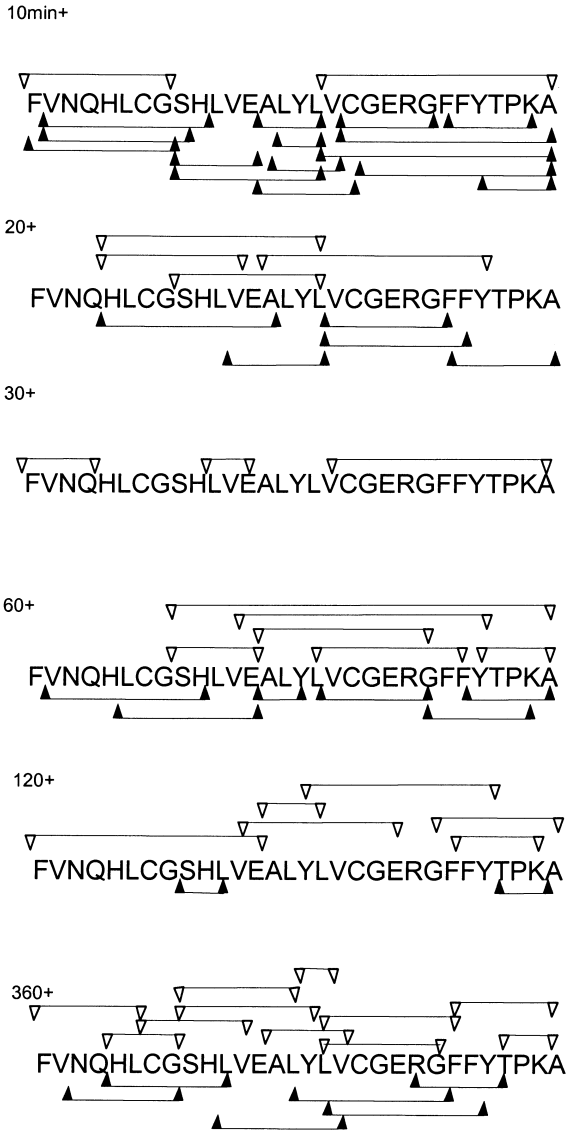

Fig. 2 Schematic representation of B_{ox} degradation by r20S*Mj*p. *Open and solid triangles* represent the unambiguous MS identification of fragments generated at 35° and 75°C, respectively. Fragments appeared in the degradation TIC only after the times indicated along the *left hand margin*

primary sequence and its orientation within the proteasome, manifest observed proteolytic cleavage specificities. In particular, hydrophobic interactions within the r20S*Tap* α-β cleft have been implicated as an important determinant in the positioning of substrates and inhibitors in the active-site chamber (Akopian et al. 1997). Thus, increased hydrophobic interactions within the proteasome cleft induced at higher temperatures could impede the translocation of a long, locally hydrophobic polypeptide substrate (like B_{ox}), thereby reducing the hydrolysis rate for that substrate. By comparison, the binding and reactive orientation of small (1–3 residue) peptide substrates are presumably less precise, and less susceptible to restrictions imposed by the hydrophobic environment of the chamber.

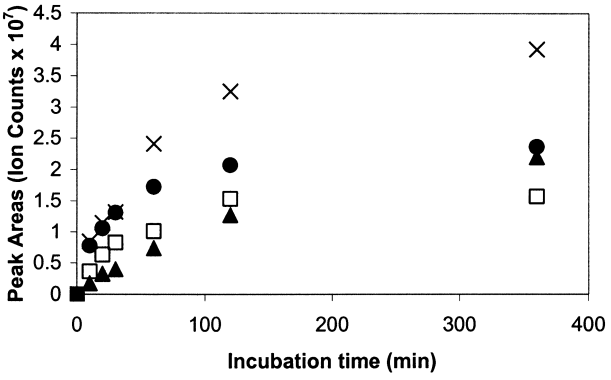

Fig. 3 Representative rate trajectories for fragments appearing in the first 10 min of incubation at 75°C. The following symbols represent the sequenced fragments and the residue numbers: ● VCGERGFFYTPKA (18–30); □ FVNQHLCG (1–8); ▲ SHLVE (9–13), and × ALYL (14–17)

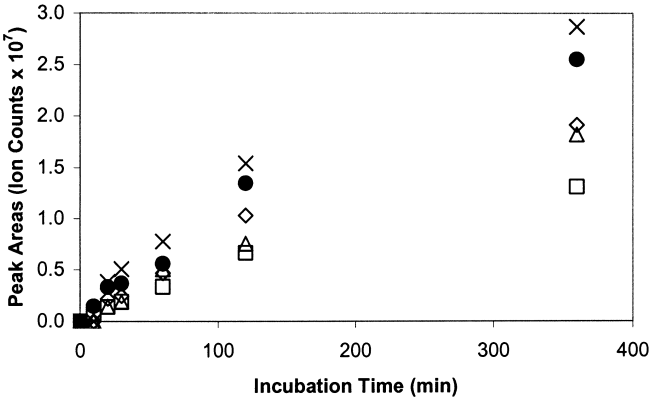

Fig. 4 Representative rate trajectories for fragments appearing in the first 20 min of incubation at 35°C. The following symbols represent the sequenced fragments and the residue numbers: ● VCGERGFFYTPKA (18–30); □ FVNQHLCG (1–8); ▲ SHLVEALYL (9–17); × HLCGSHLVEALYL (5–17), and ◇ ALYLVCGERGFFY (14–26)

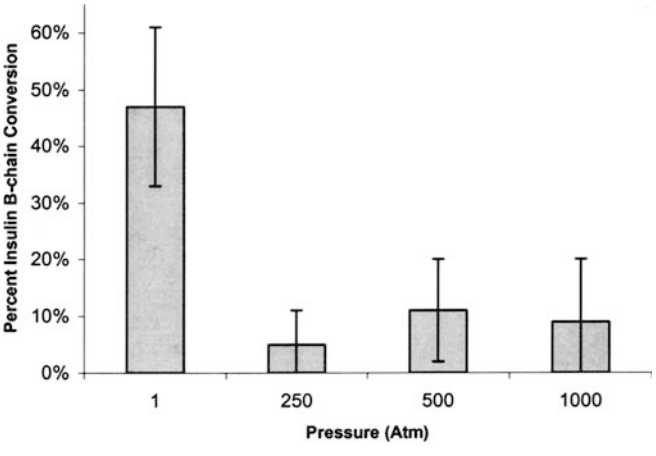

Fig. 5 Effect of hydrostatic pressure on the proteolytic conversion of B_{ox} by r20S*Mj*p. Percentage conversion was calculated from the area of the B_{ox} peak in the MS TIC at time zero and after 12 h at 35°C and the indicated pressure. The errors were determined from measurements of duplicate samples

The previously reported increased hydrolysis rate of Cbz-Ala-Ala-Leu-pNA by n20S*Mj*p at elevated pressure was most likely the result of a reduction in the overall volume of the reaction transition state and the corresponding rate enhancement associated with increased pressure (Michels and Clark 1997). Most studies demonstrating pressure activation consider the interactions of large proteins with small-molecule substrates (Miller et al. 1989; Heremans 1982) or inhibitors (Fukuda and Kunugi 1984). The apparent decrease in proteasomal activity observed for B_{ox} at high pressures may be attributable to the diversity of interactions encountered by a long substrate traversing the interior of the proteasome. For example, application of high pressure may increase the strength of hydrophobic interactions between the substrate molecule and the inner regions of the proteasome, as pressure was shown to do in previous studies of GAPDH thermostability (Hei and Clark 1994). The crystal structure of the *Ta* proteasome (Lowe et al. 1995) revealed seven hydrophobic loops extending into the α-ring orifice. This hydrophobic barrier at the proteasome's substrate access pore, in addition to hydrophobic interactions within the interior, may serve to functionally impede the translocation of substrates to the active sites. These effects could be compounded by the addition of higher pressure. The decrease in conversion of B_{ox} and the corresponding decrease in fragment production with increased pressure are consistent with this hypothesis. In this regard it is worth noting that the primary and secondary structures of proteins are generally unaffected by pressures below 5–10 kbar (Boonyaratanakornkit et al. 2002, and references therein); thus, the significant effect of pressure on B_{ox} hydrolysis at 250–1,000 atm is unlikely to be the result of pressure-dependent changes in the structure of the substrate.

Cleavage specificities of r20S*Mj*p

The observed proteolytic products and specificities for the r20S*Mj*p against B_{ox} are consistent with the findings for r20S*Ta*p (Wenzel et al. 1994) and human red blood cell proteasomes (macropain) (Dick et al. 1991) (see Fig. 6). The hydrolysis of the C_7–G_8 peptide bond represents the only cleavage unique to r20S*Mj*p. That the cleavage patterns for the two archaeal proteasomes are similar is not surprising; however, the cleavage similarities to human macropain are unexpected due to the variety of β-subunits available in eukaryotic systems. On the other hand, the absence of several activities appears to have been maintained in the evolution of the proteasome. For example, the cleavage of N_3–Q_4 and P_{28}–K_{29} peptide bonds in B_{ox} has not been observed regardless of species (Fig. 6).

Similar numbers of peptide fragments were produced in B_{ox} degradation reactions with the r20S*Ta*p and r20S*Mj*p (Table 3). Wenzel et al. (1994) found that the majority of the smaller fragments (< 7mers) produced by r20S*Ta*p were derived from the N-terminal end of B_{ox}; however, the majority of the smaller fragments produced by r20S*Mj*p were generated from the C-terminal end. The size distribution of peptides observed by Wenzel et al. (1994) evoked the molecular ruler concept, whereby two active sites act in concert. The appearance of VCGERGFFYTPKA (18–30) and ALYL (14–17) at similar rates suggests that concerted cleavage is also probable for r20S*Mj*p, although the short length of ALYL is difficult to reconcile with a concerted cleavage mechanism and the shortest distance (2 nm) between active sites estimated by Wenzel et al. (1994). Moreover, generation of ALYL was not observed at 35°C (Fig. 4), suggesting that additional substrate interactions within the proteasome at higher temperatures influence concerted cleavage. These interactions may also contribute to the delayed release of several fragments created by high-rate cleavages. For example, at 75°C one would expect to see similar production rates for FVNQHLCG (1–8) and SHLVE (9–13) resulting from a G_8–S_9 cleavage of FVNQHLCGSHLVE (1–13); however, the appearance of SHLVE (9–13) is delayed.

Fig. 6 Comparison of the observed cleavages of B_{ox} by r20S*Mj*p (this report), r20S*Ta*p (Wilson et al. 2000), and human macropain (Dick et al. 1991). *Large triangles* represent primary cleavage sites and *smaller triangles* represent secondary cleavages. Relative cleavage specificities were not determined for r20S*Ta*p. Several additional cleavage fragments were observed for human macropain at long incubation times (> 20 h), but cleavage sites were not determined

From a physiological perspective, high thermotolerance of the proteasome is expected given the deep-sea hydrothermal habitat of *Mj*, in which the organism may experience wide variations in temperature, including at least brief exposures to supraoptimal growth temperatures. The apparent pressure inhibition of the proteasome is more surprising, especially in view of the previously reported barophilic growth response of *Mj* (Michels and Clark 1997) and the pressure activation of its hydrogenase (Miller et al. 1989). Perhaps the lower proteasome activity at the in situ pressure is part of a regulatory mechanism that confers some advantage to the cell. A more complete understanding of temperature-pressure relationships in the physiology of *Mj* and the functional properties of its enzymes awaits further investigation.

Acknowledgments This research was supported by the Bayer Corparation, UCSF/NIGMS (R25GM6847-02), NSF (BES-0224733), the Schlumberger Fellowship of DSC, and the Kyowa Hakko Kogyo Co. The authors would like to thank Michael Ru for his assistance in preparing the manuscript, and the following for their helpful contributions: David Altreuter, Tina Hsu, Richard Carrillo, and Peter Zwickl.

References

Akopian TN, Kisselev AF, Goldberg AL (1997) Processive degradation of proteins and other catalytic properties of the proteasome from *Thermoplasma acidophilum*. J Biol Chem 272:1791–1798

Boonyaratanakornkit BB, Park CB, Clark DS (2002) Pressure effects on intra- and intermolecular interactions within proteins. Biochim Biophys Acta 1595:235–249

Chen P, Hochstrasser M (1995) Biogenesis, structure and function of the yeast 20S proteasome. EMBO J 14:2620–2630

Dick LR, Moomaw CR, DeMartino GN, Slaughter CA (1991) Degradation of oxidized insulin B-chain by the multiproteinase complex macropain (proteasome). Biochemistry 30:2725–2734

Djaballah H, Rowe AJ, Harding SE, Rivett AJ (1993) The multicatalytic proteinase complex (proteasome): structure and conformational changes associated with changes in proteolytic activity. Biochem J 292:857–862

Frankenberg RJ, Hsu TS, Yakota, H, Kim R, Clark DS (2001) Chemical denaturation and elevated folding temperatures are required for wild-type activity and stability of recombinant *Methanococcus jannaschii* 20S proteasome. Protein Sci 10:1887–1896

Fukuda M, Kunugi S (1984) Pressure dependence of thermolysin catalysis. Eur J Biochem 142:565–70

Hei DJ, Clark DS (1994) Pressure stabilization of proteins from extreme thermophiles. Appl Environ Microbiol 60:932–939

Heremans K (1982) High pressure effects on proteins and other biomolecules. Annu Rev Biophys Bioeng 11:1–21

Kisselev AF, Akopian TN, Castillo V, Goldberg AL (1999) Proteasome active sites allosterically regulate each other, suggesting a cyclical bite-chew mechanism for protein breakdown. Mol Cell 4:395-402

Lowe J, Stock D, Jap B, Zwickl P, Baumeister W, Huber R (1995) Crystal structure of the 20S proteasome from the archaeon *T. acidophilum* at 3.4A resolution. Science 268:533–539

Maupin-Furlow JA, Aldrich HC, Ferry JG (1998) Biochemical characterization of the 20S proteasome from the methanoarchaeon *Methanosarcina thermophila*. J Bact 180:1480–1487

McGuire MJ, DeMartino GN (1989) The latent form of macropain (high molecular-weight multicatalytic protease restores ATP dependent proteolysis to soluble extracts of BHK fibroblasts pre treated with anti-macropain antibodies. Biochem Biophys Res Comm 160:911–916

Michels PC, Clark DS (1997) Pressure enhanced activity and stability of a hyperthermophilic protease from a deep sea methanogen. Appl Environ Microbiol 63:3985–3991

Miller JF, Nelson CM, Ludlow JM, Shah NN, Clark DS (1988) Pressure and temperature effects on growth and methane production of the extreme thermophile *Methanococcus jannaschii*. Appl Environ Microbiol 54:3039–3042

Miller JF, Shah NN, Nelson CM, Ludlow JM, Clark DS (1989) High pressure-temperature bioreactor: assays of thermostable hydrogenase with fiber optics. Biotechnol Bioeng 34:1015–1021

Murakami Y, Matsufuji S, Kamenji T, Hayashi S, Igarashi K, Tamura T, Tanaka K, Ichihara A (1992) Ornithine decarboxylase is degraded by the 26S-proteasome without ubiquitination. Nature 360:597–599

Rubin DM, Finley D (1995) The proteasome: a protein-degrading organelle? Curr Biol 5:854–858

Seufert W, Jentsch S (1992) In vivo function of the proteasome in the ubiquiting pathway. EMBO J 11:3077–3080

Wilson HL, Ou MS, Aldrich HC, Maupin-Furlow JA (2000) Biochemical and physical properties of the *Methanococcus jannaschii* 20S proteasome and PAN, a homolog of the ATPase (Rpt) subunits of the eucaryal 26S proteasome. J Bacteriol 182:1680–1692

Wenzel T, Eckerskorn C, Lottspeich F, Baumeister W (1994) Existence of a molecular ruler in proteasomes suggested by the analysis of degradation products. FEBS Lett 349:205–209

Yamada S, Hojo K, Yoshimura H, Ishikawa K (1995) Reaction of 20S proteasome: shift of SDS-dependent activation by divalent cations. J Biochem 117:1162–1169

Yamada S, Sato K, Yamada J, Yasutomi M, Tokumoto T, Ishikawa K (1998) Activation of the 20S proteasome of *Xenopus* oocytes by SDS: evidence for the substrate-induced conformational change characteristic of trypsin-like peptidase. Zool Sci 115:353–357

Zwickl P, Grziwa A, Puhler G, Dahlmann B, Lottspeich F, Baumeister W (1992) Structure of the *Thermoplasma* proteasome and its implications for the function and evolution of the multicatalytic proteinase. Biochemistry 31:964–972